Soil Dynamics and Earthquake Engineering 97 (2017) 277–288

Contents lists available at ScienceDirect

Soil Dynamics and Earthquake Engineering

journal homepage: www.elsevier.com/locate/soildyn

Simplified probabilistic seismic assessment of RC frames with added viscous dampers

Luca Landi*, Cristina Vorabbi, Omar Fabbri, Pier Paolo Diotallevi

Department DICAM, University of Bologna, Bologna, Italy

ARTICLE INFO

Keywords:
Nonlinear fluid viscous dampers
Nonlinear dynamic analysis
Probabilistic method
Median
Dispersion
SAC-FEMA

ABSTRACT

The object of this paper is the study of simplified probabilistic procedures for the seismic assessment of nonlinear structures equipped with nonlinear fluid viscous dampers. The considered reference probabilistic approach is the SAC-FEMA method, which allows to obtain the probability of exceeding a given performance level. The specific purpose is to study the correlation between the results obtained through the probabilistic seismic assessment method for structures with and without dampers, with emphasis on these results in terms of dispersion. A wide set of recorded ground motions was therefore selected and applied to the considered RC frames. The study was performed without applying scaling factors to the earthquake records, but by selecting different sets of records for increasing values of seismic intensity. All the obtained results were examined considering different criteria, in order to determine the set of time-history analyses to be used for the probabilistic evaluation. Different methods were then applied to obtain the dispersion of the seismic demand. With reference to the application of the SAC-FEMA method, a sensitivity analysis was also performed, considering different procedures to interpolate the hazard curve. From the analyses, it was possible to derive the expressions that allow the results for structures with and without dampers to be correlated, as well as to offer suggestions for applying the SAC-FEMA method. A second purpose of the paper is to propose and apply, in the probabilistic assessment, a direct procedure. This procedure was recently presented by some of the authors as a method to be used for obtaining the response of nonlinear structures with nonlinear viscous dampers as an alternative to expensive nonlinear dynamic analyses.

1. Introduction

Over the past fifty years, a large part of research has been dedicated to earthquake-resistant systems developed to raise seismic performance levels while keeping construction costs within reasonable levels. This aspect is particularly evident in the case of existing buildings that are unable to satisfy the seismic requirements provided by current codes. The retrofit objective of satisfying the seismic requirements of new structures is often economically prohibitive and very difficult to achieve. In these cases an innovative technique as the dissipation of energy by added damping devices may be very promising in improving the seismic performance [1–12]. In rehabilitation interventions, fluid-viscous dampers offer some advantages [3,4], as their behaviour is independent of frequency and their dissipative capacity is very high.

Performance-Based Earthquake Engineering (PBEE) is a framework used to identify and define desired structural performances for specified seismic intensity levels. Currently, the most advanced PBEE methodologies, such as the PEER PBEE procedure [13,14], have been developed to evaluate seismic performance in terms of expected economic losses, a parameter of particular interest to decision makers. The PEER PBEE procedure consists of four steps of analysis: hazard analysis for the specific site of the building, structural analysis, damage analysis and loss analysis. In all the steps, the related uncertainties are explicitly considered in a probabilistic manner. The second step, in particular, involves a series of nonlinear time-history analyses executed to obtain a probabilistic description of the seismic demand for the building at increasing seismic intensity levels.

In this framework, the widespread probabilistic SAC-FEMA approach [15] can be useful for developing simplified procedures [16,17]. This method provides a closed form expression for evaluating the annual probability of exceeding a given limit state, while accounting for record-to-record variability and modelling uncertainties. The method is based on the first two steps in the PBEE process, hazard analysis and structural analysis, and, in general, it requires a series of nonlinear time-history analyses to be performed. This probabilistic approach has been followed in the present study. The purpose of this paper is to

* Corresponding author.
E-mail address: l.landi@unibo.it (L. Landi).

http://dx.doi.org/10.1016/j.soildyn.2017.03.003
Received 5 August 2016; Received in revised form 31 January 2017; Accepted 3 March 2017

study the correlation between the results of the probabilistic assessment method for structures with and without dampers, with particular emphasis on the results in terms of dispersion caused by ground motion variability. This paper has studied, in particular, the variability and influence of the parameters in the closed form expression, such as the dispersion of seismic demand. This research takes into account the near collapse limit state, a wide set of ground motions and different methods to approximate the hazard curves. The analyses were performed without applying scaling factors to the earthquake records, and different records for increasing values of seismic intensity were instead used.

Considering the current trend of developing simplified procedures to assess performance while avoiding expensive nonlinear time-history analyses, a second purpose of the paper is to apply a direct procedure for assessing the response of nonlinear structures with nonlinear viscous dampers. This procedure was recently proposed by some of the authors and was applied within the considered probabilistic approach. Entitled DAM (direct assessment method) [18], this procedure requires knowing only the pushover curve of the structure, and it can also be applied to derive the response for increasing values of seismic intensity (IDAM). The idea was to apply this procedure in place of costly nonlinear dynamic analyses to estimate the engineering demand parameters that are needed in the SAC-FEMA approach. When simplified assessment methods are used in the place of nonlinear time-history analyses, it becomes necessary to solve the issue of uncertainties, such as record-to-record variability. A possible solution can be to use the default dispersion values available in literature [14,16]. The results of the correlation study performed as the first objective of this research can give useful indications for the specific case of existing structures retrofitted with viscous dampers. Here, when applying the probabilistic assessment together with DAM, the values obtained from the nonlinear dynamic analyses were adopted as the values of the dispersion.

The case study considered is a typical RC frame, with three bays and six floors, designed to resist gravity loads only. Nonlinear fluid viscous dampers were inserted for the seismic retrofit. The seismic demand parameters here considered are the maximum displacement at the top of the structure and the maximum inter-storey drift. Nine return periods were chosen to identify nine values for seismic intensity and twenty ground motions were selected for each. The analyses reported consider two different models for the behaviour of the plastic hinges, where the first model includes post-peak strength deterioration and the second does not. In the first case, the results were elaborated only for the records where the analyses converged for both structures. In the second case, the results were elaborated for all the considered records, that is, all 180 records for each structure.

2. Probabilistic approach

The SAC-FEMA method [15] provided the basis for the FEMA350 [19] guidelines in the structural design of steel moment-resisting frames under seismic action and can be used to determine the probability of failure for a structure in a closed form. This method specifies a closed form expression for evaluating the seismic risk of a structure in terms of P_{PL}, the annual probability of exceeding a specified performance level (e.g. the annual probability of collapse or the annual probability of exceeding the life safety level). Three approximations were proposed to obtain a closed form expression for P_{PL}, one for the probabilistic representation of ground motion intensity, one for displacement demand and one for displacement capacity. For the first approximation, the assumption is that the site hazard curve can be approximated in the region of hazard levels close to the limit state probability P_{PL} through the following relationship:

$$H(S_a) = k_0 S_a^{-k_1} \tag{1}$$

where $H(S_a)$ is the annual probability of exceeding S_a, S_a is the spectral acceleration at the fundamental period (assumed as the intensity measure), and k_1 and k_0 are constants that depend upon the interpolation of the hazard function in a log-log plot in the region of interest. For the second approximation, the assumption is that the median drift demand $\hat{D}$ can be represented by the following relationship:

$$\hat{D} = a(S_a)^b \tag{2}$$

where a and b are constants that depend upon the interpolation of the results in terms of seismic demand. Lastly, for the third approximation, the assumption is that the drift demand D is lognormally distributed about the median, using the standard deviation of the natural logarithm, $\beta_{D|Sa}$. This will be considered as the definition of dispersion. In addition, the drift capacity C is assumed to be lognormally distributed with dispersion β_C. Using the previous approximations, it is possible to derive the following expression:

$$P_{PL} = H(S_{a,1}^{\hat{C}}) \exp\left[\frac{1}{2}\frac{k_1^2}{b^2}\left(\beta_{D|S_a}^2 + \beta_C^2\right)\right] \tag{3}$$

where $S_{a,1}^{\hat{C}}$ is the spectral acceleration associated to attaining the drift capacity. From Eq. (3), it can be seen that the record-to-record variability and modelling uncertainties are able to affect P_{PL} through the exponential correction factor.

3. Direct Assessment Method (DAM) for nonlinear structures equipped with nonlinear viscous dampers

The DAM procedure, recently proposed and verified by some of the authors [18], was applied in this research as an alternative to nonlinear dynamic analyses. For completeness, it is explained here very briefly and, for more details, see Ref. [18]. The procedure consists of two steps.

The first step is used to obtain the direct estimate of the supplemental damping provided by the nonlinear viscous dampers applied to a linear elastic structure. In the case of nonlinear viscous dampers, the supplemental damping is dependent on the structural response. Therefore, a new dimensionless parameter is introduced for both the single (SDOF) and the multi-degree-of-freedom (MDOF) systems. This parameter is called the damper index [20] and it does not depend on the structural response. If a MDOF system is considered, the damper index for the first mode can be defined as:

$$\varepsilon_1 = \frac{T_1^{\alpha}\lambda \sum_{j=1}^{N_D} c_{NLj} f_j^{1+\alpha} \phi_{rj1}^{1+\alpha}}{(2\pi)^{1+\alpha}(\Gamma_1 \ddot{u}_{g0})^{1-\alpha} \sum_{i=1}^{N} m_i \phi_{i1}^2} \tag{4}$$

where c_{NLj} is the damping coefficient, λ is a constant depending on the exponent of velocity α, N_D and N are, respectively, the number of devices and degrees of freedom (DOF), f_j is an amplification factor related to the geometrical arrangement of the damper and T_1 is the elastic period of the first mode of vibration. In addition, ϕ_{rj1} is the difference between the first modal ordinates associated with the DOFs j and j-1, Γ_1 is the first modal participation factor, $\ddot{u}_{g0}$ is the peak ground acceleration (PGA) and m_i is the mass of the DOF i. In general, the damper index ε and the supplemental damping under elastic condition ξ_{ve} can be related through the following equation:

$$\xi_{ve} = \varepsilon \cdot [\overline{S}_a(T, \xi_{ve})]^{\alpha - 1} \tag{5}$$

where $\overline{S}_a$ is the spectral acceleration normalized to the PGA. Once the damper index is known, it is possible to calculate the supplemental damping ξ_{ve} using particular spectra of the supplemental damping as a function of the elastic period, for constant values of the damper index. These spectra can be obtained by applying Eq. (5) once the spectrum of the seismic action is known. They can, specifically, be derived on the basis of the code spectrum.

The second step of the DAM extends the procedure to consider the nonlinear behaviour of a structure. Once the pushover curve of the structure is known, an effective period T_{eff} can be associated to the SDOF system that is equivalent to the actual structure. The damping reduction factor B of the spectral ordinates can be determined through the following equation:

$$B(\xi_{eff}) = \frac{S_{a,el}(T_{eff})}{S_{ay}} = \frac{S_{a,el}(T\sqrt{\mu_D})}{S_{ay}} \tag{6}$$

where $S_{a,\,el}$ is the elastic demand in terms of acceleration, μ_D is the ductility demand and S_{ay} is the maximum level of acceleration that the structure can bear. Eq. (6) also shows that the damping reduction factor is a function of the effective damping ξ_{eff}, which is the total damping of the equivalent SDOF system. By inverting Eq. (6), it is possible to obtain a curve, called constant capacity damping curve, that correlates the effective damping with the ductility demand (unknowns of the problem) for a given value of the fundamental elastic period. Another relationship between the effective damping and the ductility demand can be derived by studying the damping properties of the structural system with the damping devices, for a given value of the supplemental damping ξ_{ve} (output of the first step):

$$\xi_{eff} = \xi_i + \frac{C}{\pi}\left(1 - \frac{1}{\mu_D}\right) + \xi_{ve}(\mu_D)^{1-\frac{\alpha}{2}} \tag{7}$$

where ξ_i is the inherent damping, the second term is the hysteretic damping in the case of elastic-plastic monotonic response and the third is the supplemental damping caused by nonlinear viscous dampers in the presence of nonlinear structural behaviour. The parameter C depends on the type of hysteretic response of the structure. If the supplemental damping ξ_{ve} and the yield acceleration S_{ay} are known, it is possible to identify the two curves mentioned and to assess directly both the ductility demand and the effective damping as their intersection point (Fig. 1).

As explained in the introduction, the DAM procedure can be used in place of nonlinear time-history analyses to determine approximated curves representing the selected engineering demand parameters as functions of seismic intensity. The method is applied by repeating the two steps for increasing values of the seismic intensity of the considered spectrum (IDAM).

4. The considered case study

The case study considered is a configuration that represents typical RC frames, with three bays and six floors (Fig. 2). This frame was designed only to resist gravity loads. Nonlinear fluid viscous dampers were inserted to increase the level of seismic action bearable by the structure. The properties of the dampers, obtained with design

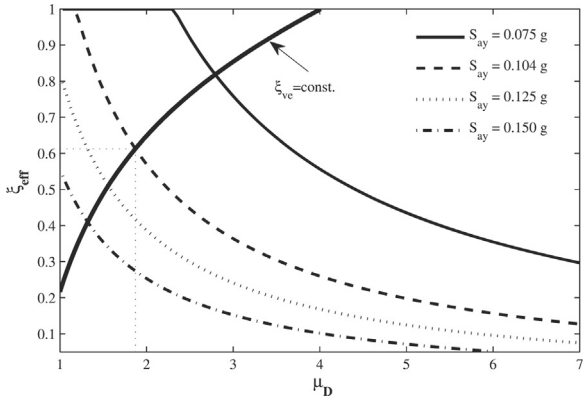

Fig. 1. Constant capacity damping curves (for a given T_1) and constant supplemental damping curve in terms of ductility demand [18].

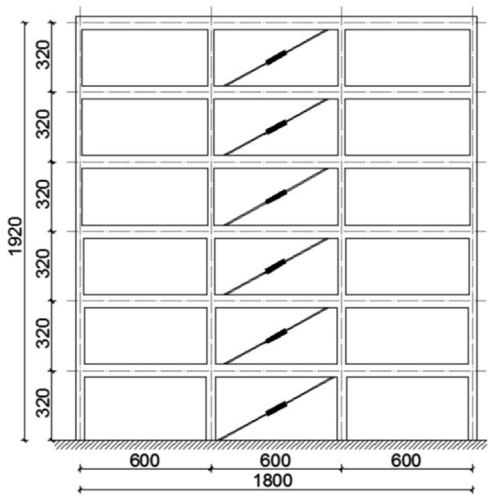

Fig. 2. Geometrical characteristics of the considered RC frame (dimensions in cm).

methods previously presented [10,12], were taken as given parameters in this paper. They are the exponent of velocity α=0.5, the supplemental damping provided by the damping system equal to 24.5% and the damping coefficient equal to 556 kN $(s/m)^{0.5}$. Regarding the geometry of the structure, each bay is 6 m wide and each inter-storey is 3.2 m high. The beams are 30 cm wide and 60 cm deep on all floors. The columns have a square cross section. On the ground floor, the columns at the edge of the building have a length of 40 cm, while the central columns have a length of 45 cm. All columns have a square cross section, on the first floor of 40×40 cm, on the third floor, of 35×35 cm and on the last three floors, of 30×30 cm. Concrete with a cylinder strength of 28 MPa and steel with a yield strength of 450 MPa have been assumed in this study. The seismic weights are 516.6 kN for the sixth floor, 833.4 kN for the fifth and fourth floors, 838.6 kN for the third floor, 849.8 kN for the second floor and 859.2 kN for the first floor. The structure is assumed to be located in Santa Sofia, Italy. According to the Italian building code [21], for each site, identified by its latitude and longitude, it is possible to define the different elastic response spectra for the different values of the return period T_R of the seismic action.

Since the aim of this paper is to perform the probabilistic assessment of the seismic response of RC structures equipped with nonlinear fluid viscous dampers, it was necessary to carry out a wide number of nonlinear dynamic analyses and, consequently, select a high number of spectrum-compatible recorded ground motions. Nine return periods were considered (T_R=30, 50, 101, 201, 475, 664, 975, 1950 and 2475 years). For each of them, Rexel software [22] was used to select a number of different sets containing 20 recorded ground motions with an average elastic acceleration response spectrum compatible with the code spectrum (Italian building code, [21]). The code elastic response spectrum for the assumed site and type C soil was determined for each return period considered. Given the site and the soil type, the PGA for T_R=475 was equal to 0.29g. Fig. 3 shows the spectra of the 20 selected records for T_R=475 years and their average spectrum compared to the code spectrum.

The software used to select the records, Rexel, allows different ground motion databases to be considered. The records used in the nonlinear dynamic analyses were selected from the European Strong Motion Database [23]. In this database, the ground motions were selected on the basis of their magnitude interval being between 4 and 7 and their maximum distance from the epicentre being 60 km. The rules followed for spectrum compatibility were the following. Each set of 20 records was defined so that the average of the spectra of the single records, scaled to the code PGA, was sufficiently close to the code spectrum associated to a given return period. This meant that the

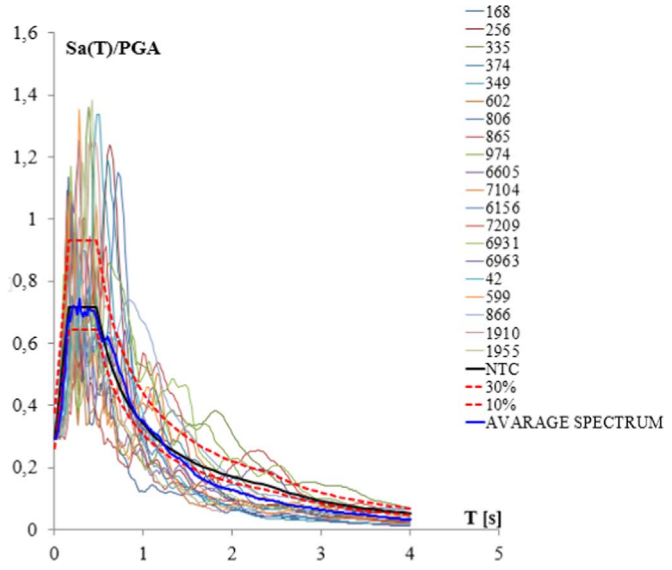

Fig. 3. Spectra of the 20 selected compatible records for T_R=475 years, average spectrum of the selected records, code spectrum and tolerance limits (30% and 10%).

average spectral acceleration of the set of records was not to be less than 10% or greater than 30% of the code spectral acceleration. In general, this condition was imposed for the interval of periods between 0.15 s and 2.0 s. However, due to the difficulty in selecting a large number of records, the upper limit was reduced for the longer return periods, but even so all the periods of interest for the analyses were included.

Nonlinear dynamic analyses were performed using a concentrated plasticity model implemented on a finite element computer program (SAP2000) [24]. A moment-rotation curve was assigned to the plastic hinges located at the ends of each element. The moment-rotation curve was identified by assigning the yielding and ultimate bending moments and the corresponding chord rotations. These values were obtained from the empirical relationships given in the Commentary to the National code [25] and inspired by those proposed by Panagiotakos and Fardis [26]. The rotation θ_u at the ultimate condition was, therefore, calculated using the following expression:

$$\theta_u = \frac{1}{\gamma_{el}} 0.016 \cdot (0.3^{\nu}) \left[\frac{\max(0.01, \omega')}{\max(0.01, \omega)} f_c \right]^{0.225} \left(\frac{L_V}{h} \right)^{0.35} 25^{\left(a_c \rho_{sx} \frac{f_{yw}}{f_c} \right)} (1.25^{100 \rho_d}) \quad (8)$$

where γ_{el} is equal to 1.5 for primary elements and to 1 for secondary elements, ν is the axial force ratio, ω and ω' are the mechanical reinforcement ratios of tension and compression reinforcements, respectively. In addition, h is the section depth, f_c is the cylinder compressive strength of concrete (in MPa), f_{yw}, is the yield stress of transverse reinforcement, ρ_{sx} is the transverse reinforcement ratio, ρ_d is the diagonal reinforcement ratio, L_V is the shear span and a_c is an efficiency factor of confinement [25]. The shear span was determined for each member through a preliminary elastic analysis under lateral loads. Once the moment-chord rotation diagram was determined, the moment-plastic rotation diagram was derived by subtracting the yielding rotation from the rotation values of the first diagram. The moment-plastic rotation diagram was then assigned to the set of properties for each plastic hinge as the relevant monotonic moment-rotation law. The flexural strength and deformation capacity of the columns were calculated taking the effect of the axial forces into account. The interaction between the flexural strength and the axial force was considered by calculating the flexural strength for different given values of axial force and through interpolation for the other values of axial force. The effect of the axial force on the deformation

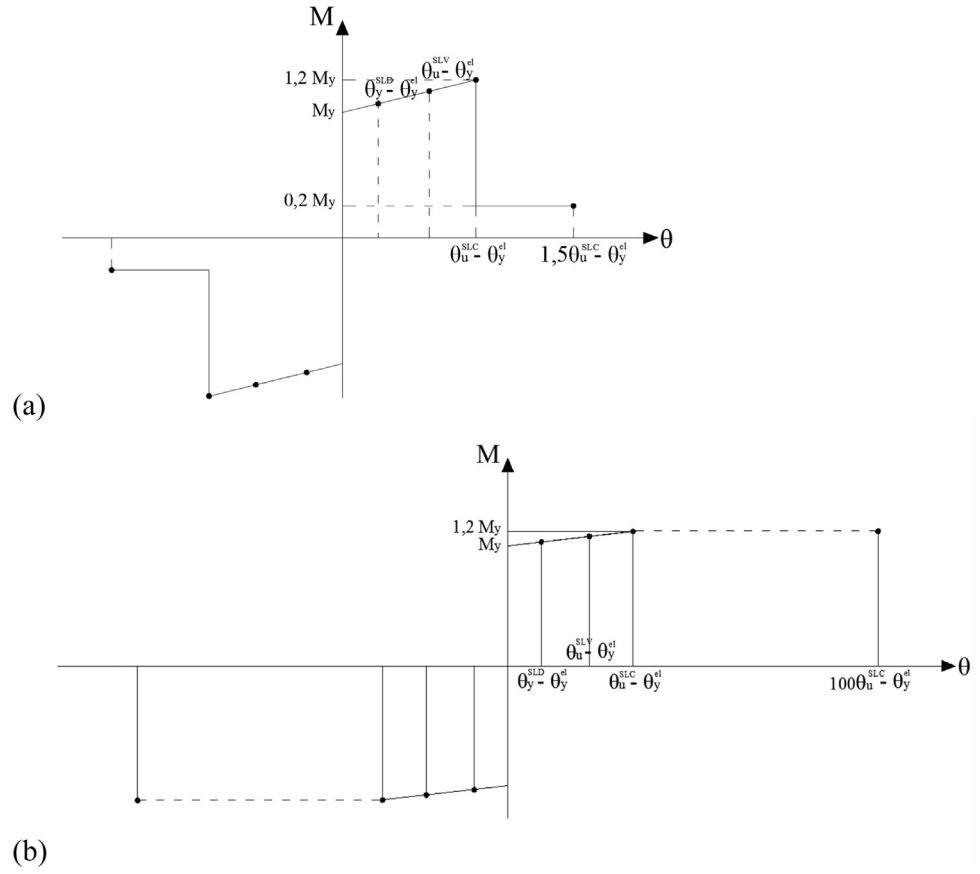

Fig. 4. Moment-rotation diagrams assigned to plastic hinges: a) trilinear curve with post peak strength deterioration; b) bilinear curve without strength deterioration.

Table 1
The three cases in which the performed analyses have been grouped.

	Case 1) Trilinear moment-rotation curve with post peak strength deterioration	Case 2) Trilinear moment-rotation curve with post peak strength deterioration	Case 3) Bilinear moment-rotation curve without post peak strength deterioration
Structure with dampers	170 results	104 results	180 results
Structure without dampers	104 results	104 results	180 results

capacity was taken into account by applying Eq. (8) and specifically through the axial force ratio v.

Two different moment-rotation curves were considered. A moment-rotation curve with post peak strength deterioration was initially used (trilinear moment rotation curve, Fig. 4a). Subsequently, a moment-rotation curve without post-peak strength deterioration (bilinear moment-rotation curve, Fig. 4b) was considered to ease the convergence of a large number of analyses, especially since nonlinear viscous dampers were present together with nonlinear RC elements. This also meant that it was possible to obtain a greater number of results for the probabilistic assessment.

Various reasons were behind the choice of considering the two moment-rotation curves shown in Fig. 4, instead of a curve with gradual strength deterioration. Firstly, the two diagrams in Figs. 4a and b represent the two limit conditions compared to the case of gradual deterioration. The diagram in Fig. 4a, showing sudden deterioration, means that it may be possible to exclude the cases in which the ultimate rotation is exceeded. On the other hand, according to the diagram in Fig. 4b, it may be possible to consider the results for all the records and seismic intensity levels, thus having the same number of results for all the intensity levels. Moreover, for the maximum intensity levels, in most cases, the plastic rotations obtained were not much greater than the ultimate rotations. It follows that, by assuming gradual deterioration in place of the diagram in Fig. 4b, this should not affect the results in a significant way.

The obtained results were then grouped into three cases, as shown in Table 1. In the first case, the trilinear moment rotation curve (Fig. 4a) was considered and the probabilistic assessment was carried out on 170 and 104 records for the structure with and without dampers, respectively. These were the records where the analyses converged. In the second case, the plastic hinge model used in the first case was adopted, but the probabilistic assessment was calculated on an equal number of records, i.e. 104 for both structures. In the third case, a bilinear moment rotation curve (Fig. 4b) was assumed and the probabilistic assessment was performed on 180 records for both structures.

5. Results and comments

5.1. Probabilistic seismic demand analysis

The following parameters were examined for each nonlinear dynamic analysis:

1. Profiles of maximum displacement, obtained from the envelope of the maximum displacements which occur on each floor during the seismic event;
2. Profiles of maximum inter-storey drift, which represent the envelope of maximum inter-storey drifts occurring during the seismic event.

Having obtained the maximum displacement and maximum inter-storey drift profiles, it was possible to determine the maximum displacement at the top of the building (D_{roof}) and the maximum inter-storey drift (δ_{max}) along the height of the building for each record and each return period. The values thus obtained were plotted in graphs. These graphs contain a parameter representing seismic intensity ($S_a(T_1)$, the spectral acceleration at the first natural period of the structure with 5% damping) as the abscissa and a parameter representing seismic demand (D_{roof} or δ_{max}) as the ordinate.

The median and the dispersion values were determined in order to perform the probabilistic assessment. Regarding the median, it was assumed from the scientific literature [15] that the distribution of median values of the seismic demand parameters follows the relationship:

$$MeD = a(S_a(T_1))^b \tag{9}$$

where MeD is the median value of the demand parameter D, $S_a(T_1)$ is the spectral acceleration and a and b are constants deriving from regression analysis. These constants were identified for D_{roof} and δ_{max} once the points MeD_{roof} -$S_a(T_1)$ and $Me\delta_{max}$ -$S_a(T_1)$ were determined for each return period.

With regards to dispersion, two different dispersion formulations were considered. The first formulation considers a variable dispersion with regards to seismic intensity. The dispersion for each return period was obtained through the formulation proposed in scientific literature, standard deviation of the natural logarithm of the various demand parameters. Variable dispersion is indicated with the notation β_{regr} and was obtained through the expression:

$$\beta_{D|S_a} = \sqrt{\frac{\sum_k (\ln x_k - \hat{\mu})^2}{n}} \tag{10}$$

where n is the number of values and $\hat{\mu}$ is determined as the mean of the natural logarithm of the results:

$$\hat{\mu} = \frac{\sum_k \ln x_k}{n} \tag{11}$$

A regression analysis was carried out on the obtained dispersion values, determining the parameters of the straight line which best interpolates the dispersion values:

Table 2
Expressions of median and dispersion for D_{roof} and δ_{max}, Case 1.

D_{roof}		δ_{max}	
Structures with dampers 170 records	Structures without dampers 104 records	Structures with dampers 170 records	Structures without dampers 104 records
MeD_{roof}=0.2114·$S_a^{0.9872}$	MeD_{roof}=0.2129·$S_a^{0.8059}$	$Me\delta_{max}$=2.041· $S_a^{1.0755}$	$Me\delta_{max}$=4.1216· $S_a^{1.1327}$
β_{regr}=0.3385+0.3894S_a	β_{regr}=0.3274+0.2272S_a	β_{regr}=0.3359+0.4341S_a	β_{regr}=0.4016–0.2375S_a
β_{cost}=0.4523	β_{cost}=0.5252	β_{cost}=0.4595	β_{cost}=0.56296

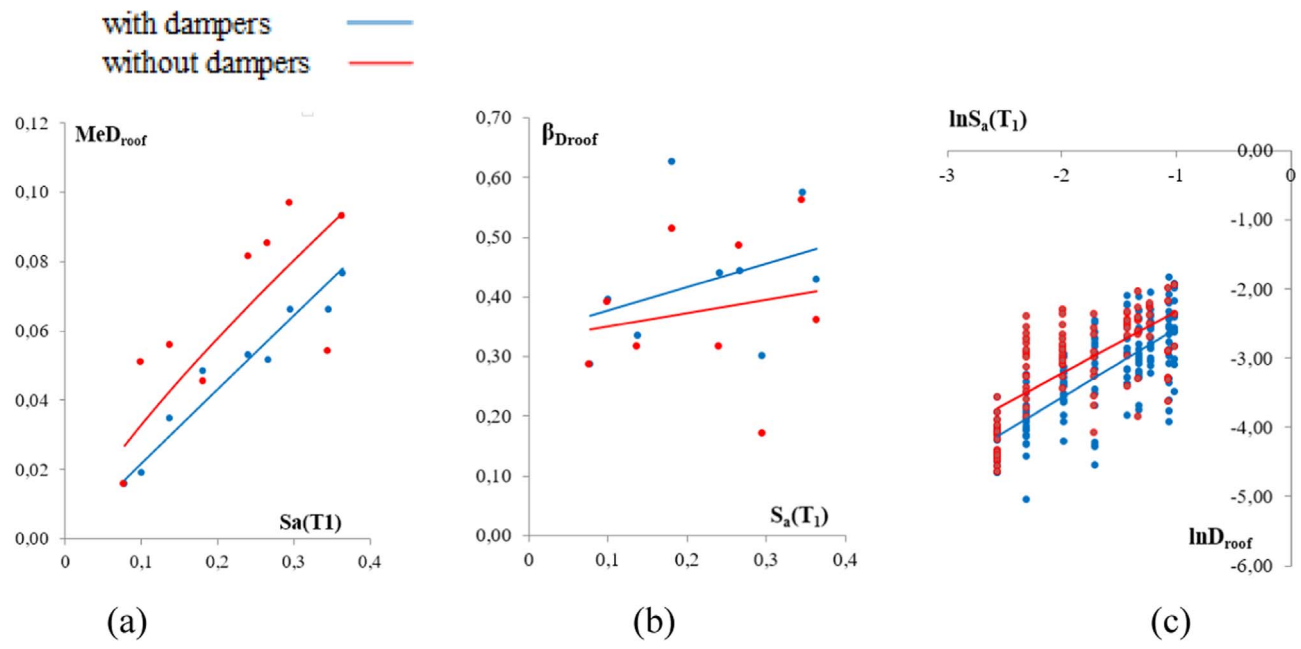

Fig. 5. Case 1: a) MeD_{roof} [m]- $S_a(T_1)$ [g]; b) βD_{roof}- $S_a(T_1)$ [g]; c) $\ln D_{roof}$- $\ln S_a(T_1)$.

$$\beta_{D|S_a} = a + bS_a(T_1) \quad (12)$$

In order to evaluate the accuracy of the obtained correlation, the parameter R^2 (determination index) and the errors (mean and standard deviation of residues) were taken into account. The second formulation, denoted by β_{cost}, considers a parameter of constant dispersion with regards to seismic intensity. This was obtained by performing a regression analysis of $\ln D$ on $\ln S_a$ on the totality of the results. The value thus obtained is the standard deviation of the residues.

Table 2 shows the expressions for the median and dispersion of the demand parameters for the analyses in Case 1 (see Table 1). For the same case, Figs. 5 and 6 illustrate the graphs for the median and dispersion of the demand parameters as a function of seismic intensity. The same results are reported in Table 3 and Figs. 7 and 8 for the analyses in Case 2, and in Table 4 and Figs. 9 and 10 for the analyses in Case 3. Fig. 5 shows that the median roof displacements (D_{roof}) of the structure without dampers are greater than those of the structure with dampers, as expected. With regards to the dispersion value (β_{regr}, Fig. 5b) for both the structures with and without dampers, this value increases with seismic intensity. Moreover, the dispersion of the structure with dampers is greater than that without dampers. This trend is not in line with the expectations. Lastly, Fig. 5c illustrates that, in accordance with Fig. 5a, the displacements of the structure with dampers are smaller than those obtained for the structure without dampers. Considering the parameter of constant dispersion (β_{cost}, Table 2), the dispersion of the structure without dampers is greater than that with dampers, a trend that is in line with expectations. With regards to Fig. 6, the same remarks can be made for the maximum inter-storey drifts (δ_{max}). In addition, it can be observed that the variable dispersion (β_{regr}) decreases for the structure without dampers when seismic intensity increases, a trend that is not in line with expectations, and that the values for constant dispersion (β_{cost}) are slightly higher than those obtained for D_{roof}. As noticed, a trend not in line with the expectations is found when the variable dispersion of the structure with dampers is greater than that without dampers (Figs. 5b and 6b) or when the variable dispersion decreases for the structure without dampers for increasing seismic intensity (Fig. 6b). This is probably due to the reduction of the number of records which allowed

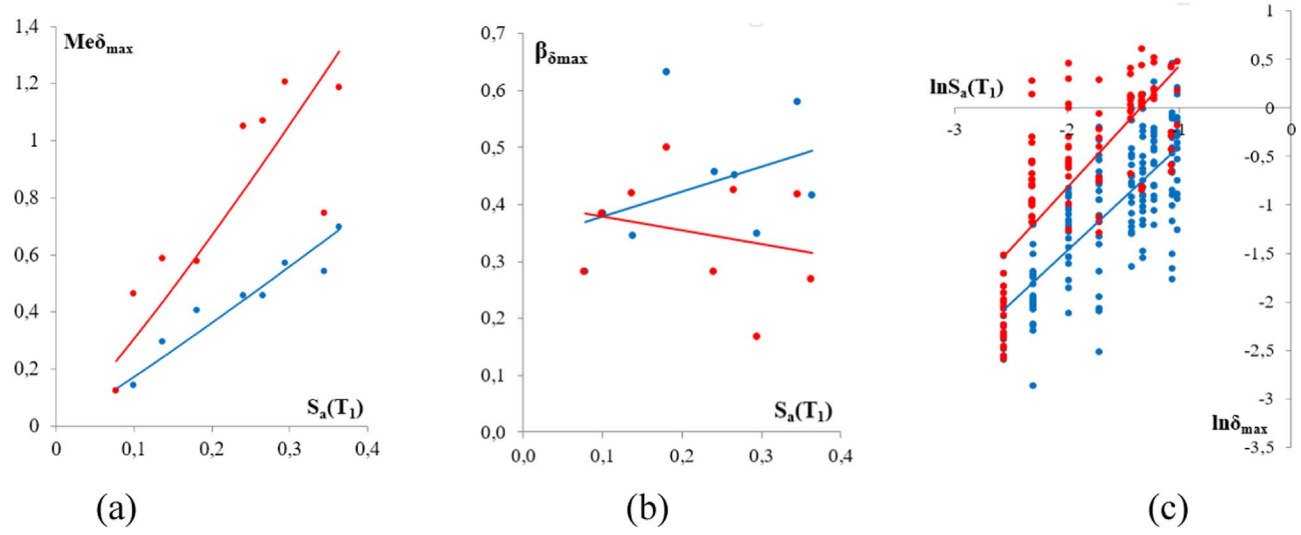

Fig. 6. Case 1: a) $Me\delta_{max}$ [%]- $S_a(T_1)$ [g]; b) $\beta\delta_{max}$- $S_a(T_1)$ [g]; c) $\ln\delta_{max}$- $\ln S_a(T_1)$.

Table 3
Expressions of median and dispersion for D_{roof} and δ_{max}, Case 2.

D_{roof}		δ_{max}	
Structures with dampers 104 records	Structures without dampers 104 records	Structures with dampers 104 records	Structures without dampers 104 records
MeD_{roof}=0.1127· $S_a^{0.7398}$ β_{regr}=0.3306+0.2143S_a β_{cost}=0.42236	$Me\delta_{max}$=0.2129· $S_a^{0.8059}$ β_{regr}=0.3274+0.2272 S_a β_{cost}=0.5252	$Me\delta_{max}$=1.0595· $S_a^{0.8221}$ β_{regr}=0.3254+0.257 S_a β_{cost}=0.42239	$Me\delta_{max}$=4.1216· $S_a^{1.1327}$ β_{regr}=0.4016−0.2375 S_a β_{cost}=0.56296

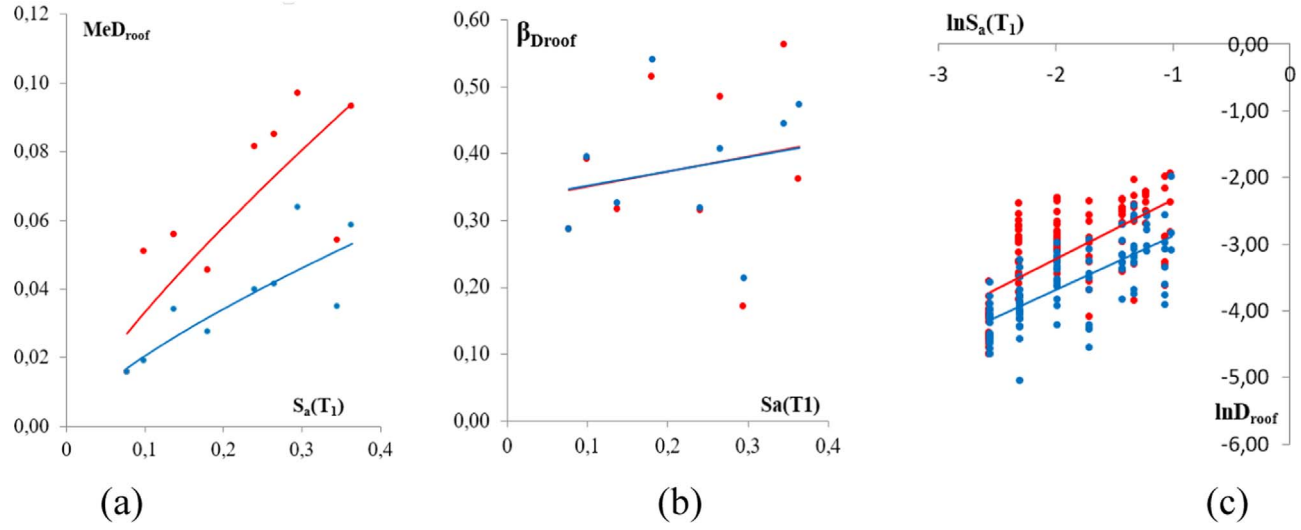

Fig. 7. Case 2: a) MeD_{roof} [m]- $S_a(T_1)$ [g]; b) βD_{roof}- $S_a(T_1)$ [g]; c) lnD_{roof}- ln$S_a(T_1)$.

to reach the convergence for the structure without dampers with the increasing of the seismic intensity, causing a reduction of the number of data and of the variable dispersion for the larger intensities.

Fig. 7a shows that, for the structure with dampers and considering Case 2 (fewer records), there are smaller values for the median D_{roof} than in Case 1. Fig. 7b confirms the fact that the dispersion (β_{regr}) always increases for both structures (with and without dampers) when the seismic intensity increases. Moreover, the values of dispersion (β_{regr}) decrease for the structure with dampers if we consider fewer records. Fig. 7c and Table 3 confirm that the trend is the same for dispersion (β_{cost}). Fig. 8 shows that the remarks regarding the maximum roof displacement (D_{roof}) can be applied to the maximum inter-storey drift. However, when passing from the structure with dampers to the one without, a trend not in line with expectations is obtained again for β_{regr}.

If we consider a greater number of records for both the structures (Case 3), the trend obtained is in line with expectations. When examining the maximum roof displacement (D_{roof}), the following observations can be made (Fig. 9). The median values for the structure without dampers are greater than those obtained for the structure with dampers (Fig. 9a). The dispersion β_{regr} always increases for both the structures when seismic intensity increases and the trend is as expected, that is the dispersion of the structure without dampers is greater than that with dampers (Fig. 9b). The dispersion β_{cost} is

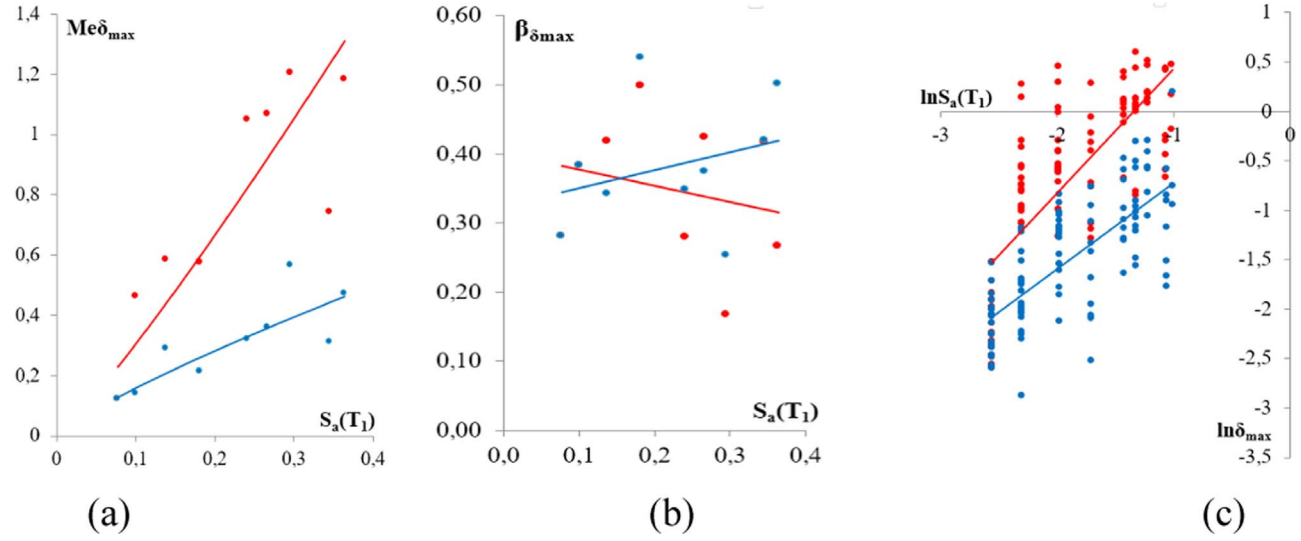

Fig. 8. Case 2: a) $Me\delta_{max}$ [%]- $S_a(T_1)$ [g]; b) $\beta\delta_{max}$- $S_a(T_1)$ [g]; c) lnδ_{max}- ln$S_a(T_1)$.

Table 4
Expressions of median and dispersion for D_{roof} and δ_{max}, Case 3.

D_{roof}		δ_{max}	
Structures with dampers 180 records	Structures without dampers 180 records	Structures with dampers 180 records	Structures without dampers 180 records
$MeD_{roof}=0.2421 \cdot S_a^{1.0523}$ $\beta_{regr}=0.3145+0.5809S_a$ $\beta_{cost}=0.4696$	$MeD_{roof}=0.44 \cdot S_a^{1.1357}$ $\beta_{regr}=0.2626+1.0257S_a$ $\beta_{cost}=0.5651$	$Me\delta_{max}=2.2724 \cdot S_a^{1.1285}$ $\beta_{regr}=0.2975+0.7001S_a$ $\beta_{cost}=0.4803$	$Me\delta_{max}=9.8605 \cdot S_a^{1.5088}$ $\beta_{regr}=0.2906+1.1428S_a$ $\beta_{cost}=0.6389$

greater for both structures than in the previous two cases, but the same trend is maintained, that is, the dispersion for the structure without dampers is greater than that for the structure with dampers (Fig. 9c). All these remarks can also apply to the maximum inter-storey drift (δ_{max}, Fig. 10), with the additional observation that the decreasing trend (observed in Cases 1 and 2) disappears for β_{regr}, which always increases with seismic intensity.

The direct assessment method [18] mentioned previously was used to estimate the median values of D_{roof} for Case 3. The method was applied using the code expression for the damping reduction factor [27], the average spectrum for each return period and the area-based criterion for the equivalent damping ratio (with C=2 in Eq. (7)). In Fig. 11, the median curves of D_{roof}, resulting from the nonlinear dynamic analyses, were compared with those obtained by applying the direct assessment method [18] for increasing seismic intensity (IDAM). It should be noted that the IDAM curves are conservative, especially for the structure with dampers. This is due to the conservative nature of the code expression used for the damping reduction factor. The IDAM curves are, in any case, consistent with the curves obtained from the nonlinear incremental dynamic analyses, confirming the effectiveness of the method as an alternative to nonlinear dynamic analyses.

Figs. 12 and 13 include the curves of the three cases presented in Table 1 for the median and the dispersion of maximum roof displacement and inter-storey drift, showing them as functions of seismic intensity. The trends described before can also be observed in these figures, where there is a clearer comparison between the different cases, i.e. between the different number of ground motions. Fig. 12 shows that the median values of D_{roof} and δ_{max} are, as expected,

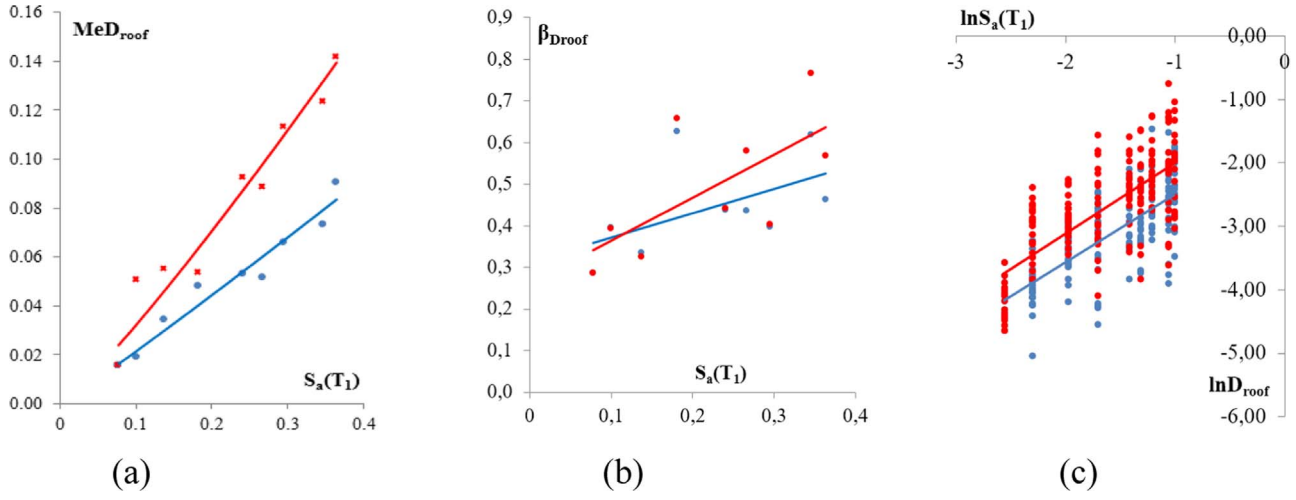

Fig. 9. Case 3: a) MeD_{roof} [m]- $S_a(T_1)$ [g]; b) βD_{roof}- $S_a(T_1)$ [g]; c) $\ln D_{roof}$- $\ln S_a(T_1)$.

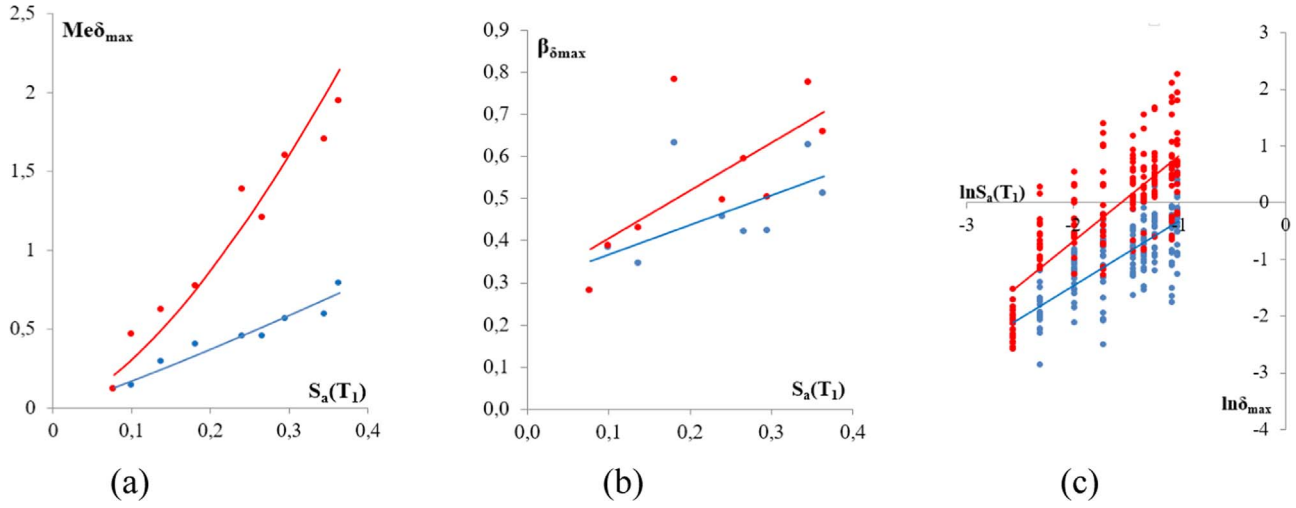

Fig. 10. Case 3: a) $Me\delta_{max}$ [%]- $S_a(T_1)$ [g]; b) $\beta\delta_{max}$- $S_a(T_1)$ [g]; c) $\ln\delta_{max}$- $\ln S_a(T_1)$.

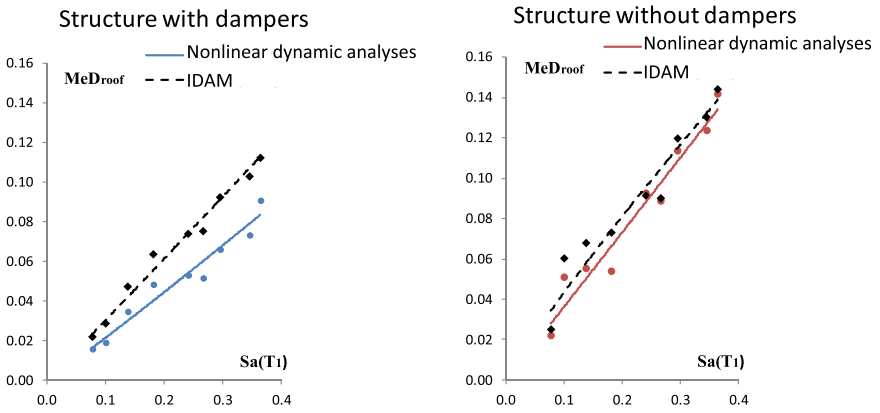

Fig. 11. Case 3: MeD_{roof} [m]- $S_a(T_1)$ [g] curves obtained with nonlinear dynamic analyses and IDAM [18].

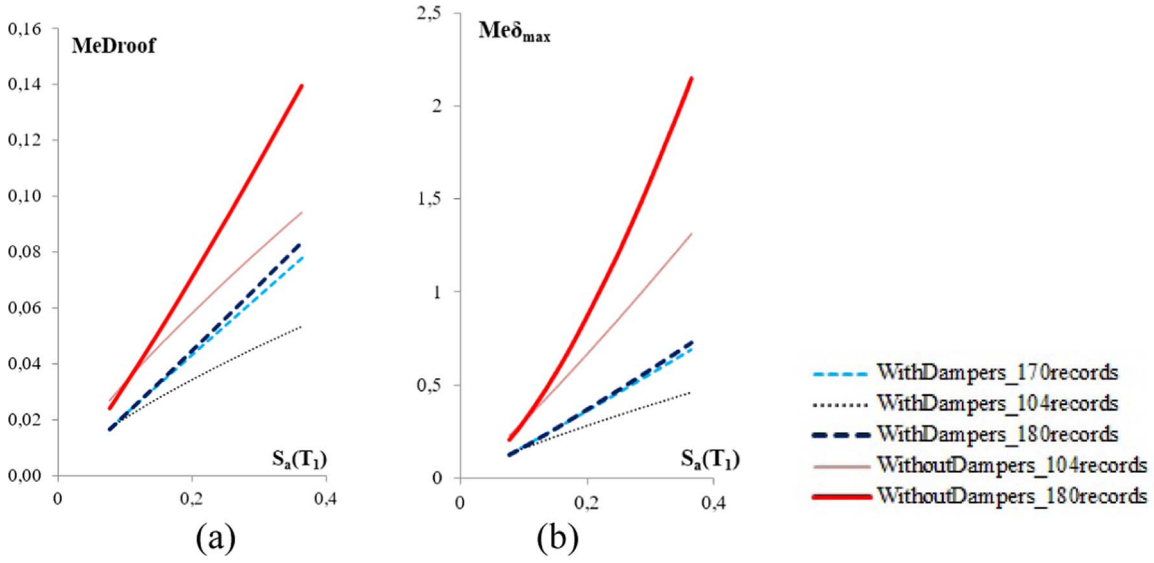

Fig. 12. Comparison between cases 1, 2 and 3: a) MeD_{roof} [m]- $S_a(T_1)$ [g]; b) $Me\delta_{max}$ [%]- $S_a(T_1)$ [g].

greater for the structure without dampers than for the structure with dampers, and that these values increase with the number of records. Fig. 13 illustrates the dispersion trend (β_{regr}). It can be seen that this dispersion increases with seismic intensity, with the exception of δ_{max} with 104 records, and that it increases with the number of records. As observed before, the expected trend is obtained for both structures with 180 records, i.e. a larger dispersion for the structure without dampers than for the structure with dampers.

Table 5 illustrates the fact that the parameter of constant dispersion (β_{cost}) increases when the number of records increases for both

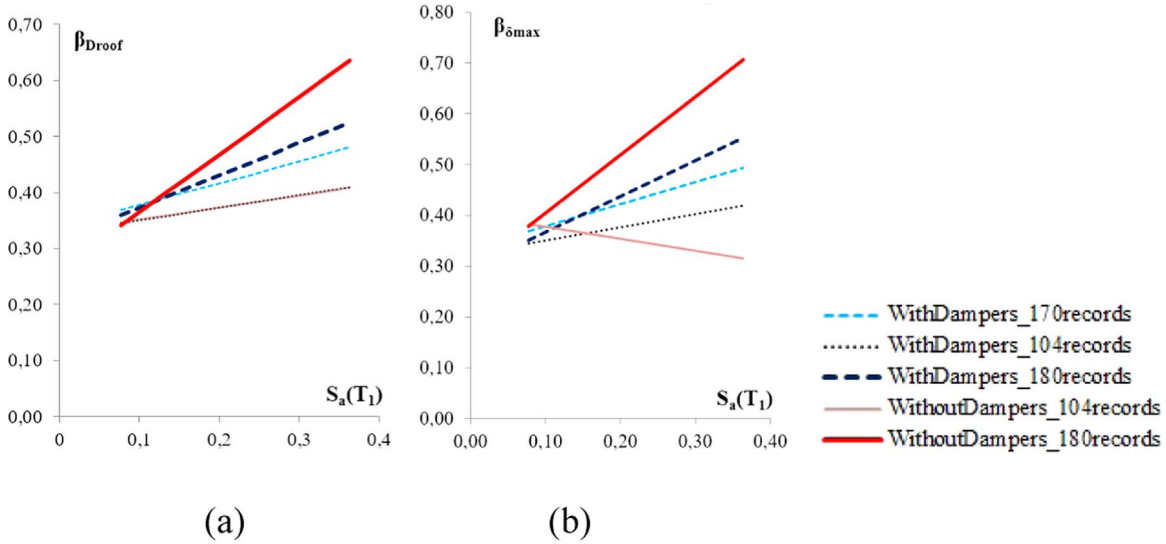

Fig. 13. Comparison between cases 1, 2 and 3: a) βD_{roof}- $S_a(T_1)$ [g]; b) $\beta\delta_{max}$- $S_a(T_1)$ [g].

Table 5
β_{cost} with the increasing of the number of records for D_{roof} and δ_{max}.

	Structure with dampers			Structure without dampers	
	104 records	170 records	180 records	104 records	180 records
$\beta_{cost}(D_{roof})$	0.42236	0.4523	0.4696	0.5252	0.5651
$\beta_{cost}(\delta_{max})$	0.42239	0.4595	0.4803	0.5629	0.6381

Table 6
$\beta_{cost,}$ ratio between the parameters of constant dispersion, obtained for the structures with and without dampers in the three cases; $\beta_{regr,}$ ratio between the coefficients of the regression lines obtained for the structures with and without dampers in the three cases.

	$\beta_{cost,\ damp}/\beta_{cost,\ withoutdamp}$				$\alpha=a_{damp}/a_{withoutdamp}$ $\lambda=b_{damp}/b_{withoutdamp}$		
	Case 1	Case 2	Case 3		Case 1	Case 2	Case 3
D_{roof}	0.8612	0.8042	0.831	α	1.714	0.943	0.566
				λ	1.034	1.009	1.198
δ_{max}	0.8162	0.7503	0.7518	α	−1.828	−1.082	0.613
				λ	0.836	0.810	1.024

structures and for both the demand parameters (D_{roof} and δ_{max}). Lastly, with regards to dispersion, it was found useful to perform some evaluations. The ratio between the parameters of constant dispersion obtained for the structures with and without dampers was calculated for the three cases. It emerged that the dispersion of the structure with dampers is about 80% that of the structure without dampers (Table 6). The ratio between the coefficients of the regression lines $\beta=a+bS_a$ obtained for the structures both with and without dampers was also calculated for the three cases. This can be used to obtain the dispersion for the structure with dampers, if that for the structure without dampers is known (Table 6). Given the previous observations concerning the dispersion trends, the most reliable correlations seem to be those obtained for Case 3, where the number of records is greater (180).

5.2. Evaluation of annual failure probability

In this section, the research focuses on studying the simplified formula proposed in the SAC-FEMA method and used to assess the annual probability of exceeding a given performance level (Eq. (3)). The study is based on the following assumptions. The near collapse (NC) limit state was taken into consideration. Different criteria for approximating the hazard curve were adopted, with interpolation performed on the entire range of return periods examined (criterion (a), T_R=30, 50, 101, 201, 475, 664, 975, 1950 and 2475 years). Interpolation was also performed on a small range close to the return period of 975 years, which in the code is associated to the near collapse limit state (criterion (b) T_R=475, 664, 975, 1950 and 2475 years). Moreover, interpolations of the first and second order were performed for both the criteria, thus identifying four hazard curves. The approximation of the second order was determined according to the method proposed by Vamvatsikos [28]:

$$H(S_a) = k_0 e^{(-k_2 \ln^2 S_a(T_1) - k_1 \ln S_a(T_1))} \tag{13}$$

where $k_1, k_2 > 0$ and $k_2 \geq 0$. Using the approximation of the second order for the hazard curve, the new closed-form expression of the annual probability of failure [28] becomes:

$$P_{F,NC} = \sqrt{p}\, k_0^{1-p} [H(S_{a,1}^{NC})]^p e^{\left(\frac{1}{2} p k_1^2 \beta_{Sc}^2\right)} \tag{14}$$

where:

$$p = \frac{1}{1 + 2k_2\beta_{Sc}^2} \quad 0 < p < 1 \tag{15}$$

The difference between Eq. (14) and Eq. (3) is the insertion of the factor p. Substituting k_2=0 in Eq. (15), it can be noted that the factor p becomes equal to unity and Eq. (14) is simplified into:

$$P_{F,NC} = [H(S_{a,1}^{NC})]^p e^{\left(\frac{1}{2} p k_1^2 \beta_{Sc}^2\right)} \tag{16}$$

The expressions of the obtained hazard curves are reported in Table 7 and the graphs of these relationships are illustrated in Fig. 14.

Table 7
Approximation of the first and second order of the hazard curve, obtained with criterion (a) and (b).

	Hazard curve criterion (a)	Hazard curve criterion (b)
1st order approximation	$H(S_a) = 3.10^{-5}(S_a)^{-2.827}$	$H(S_a) = 7.10^{-6}(S_a)^{-4.03}$
2nd order approximation	$H(S_a) = 2.62{\cdot}10^{-6} e^{(-0.878 \ln^2 S_a(T_1) - 5.923 \ln S_a(T_1))}$	$H(S_a) = 3.04{\cdot}10^{-7} e^{(-2.18 \ln^2 S_a(T_1) - 9.312 \ln S_a(T_1))}$

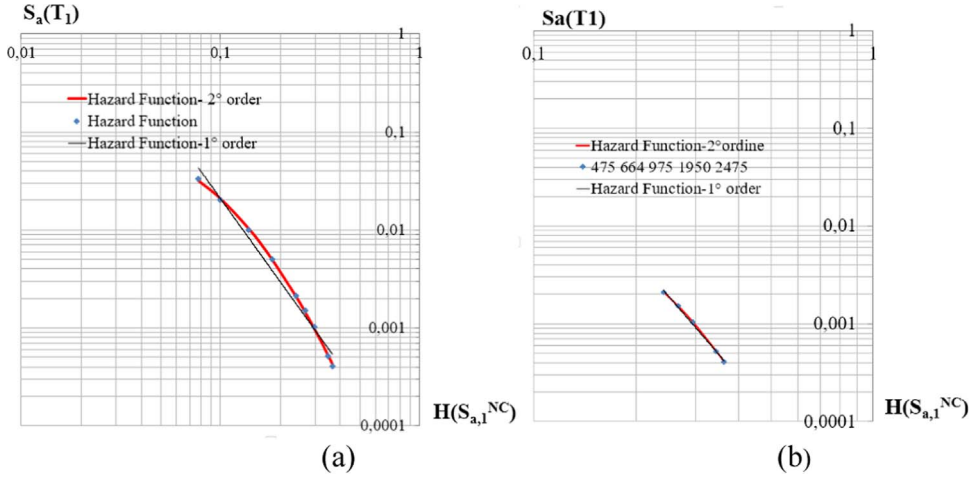

Fig. 14. Approximations of the I and II order for the hazard curve with criterion (a) and (b).

Table 8
Annual failure probability for the first order approximation of the hazard curve with criterion (a) and (b) for collapse defined by $D_{roof,u}$ ($D_{roof,u}$=0.145 m).

		Case 1		Case 2		Case 3		Case 3 (IDAM)	
		With dampers 170	Without dampers 104	With dampers 104	Without dampers 104	With dampers 180	Without dampers 180	With dampers 180	Without dampers 180
$H(S_{a,1}^{NC})$	a)	$8.8{\cdot}10^{-5}$	$1.2{\cdot}10^{-4}$	$1.2{\cdot}10^{-5}$	$1.2{\cdot}10^{-4}$	$1.2{\cdot}10^{-4}$	$4.8{\cdot}10^{-4}$	$2.6{\cdot}10^{-4}$	$2.65{\cdot}10^{-4}$
	b)	$3.3{\cdot}10^{-5}$	$4.8{\cdot}10^{-5}$	$1.8{\cdot}10^{-6}$	$4.8{\cdot}10^{-5}$	$4.9{\cdot}10^{-5}$	$3.6{\cdot}10^{-4}$	$1.53{\cdot}10^{-4}$	$1.57{\cdot}10^{-4}$
β_{regr}		0.6043	0.4686	0.6319	0.4686	0.6714	0.6486	0.585	0.6545
$P_{F,\,NC}$	a)	$5.4{\cdot}10^{-4}$	$7.1{\cdot}10^{-4}$	$3.7{\cdot}10^{-4}$	$7.1{\cdot}10^{-4}$	$7.9{\cdot}10^{-4}$	$2.2{\cdot}10^{-3}$	$1.3{\cdot}10^{-3}$	$5.55{\cdot}10^{-3}$
	b)	$1.3{\cdot}10^{-3}$	$1.9{\cdot}10^{-3}$	$2.0{\cdot}10^{-3}$	$1.9{\cdot}10^{-3}$	$2.4{\cdot}10^{-3}$	$8.2{\cdot}10^{-3}$	$5.55{\cdot}10^{-3}$	$5.43{\cdot}10^{-2}$
β_{cost}		0.4523	0.5252	0.4223	0.5252	0.4696	0.5651	0.4696	0.5651
$P_{F,\,NC}$	a)	$2.8{\cdot}10^{-4}$	$9.9{\cdot}10^{-3}$	$7.3{\cdot}10^{-5}$	$9.9{\cdot}10^{-4}$	$3.5{\cdot}10^{-4}$	$1.6{\cdot}10^{-3}$	$8.2{\cdot}10^{-4}$	$3.23{\cdot}10^{-3}$
	b)	$3.4{\cdot}10^{-4}$	$3.8{\cdot}10^{-3}$	$7.7{\cdot}10^{-5}$	$3.8{\cdot}10^{-3}$	$4.4{\cdot}10^{-4}$	$4.3{\cdot}10^{-3}$	$1.56{\cdot}10^{-3}$	$1.81{\cdot}10^{-2}$

Lastly, the determination of the capacity values for the near collapse limit state and for the two demand parameters under consideration was carried out according to two criteria described in the following. Two collapse conditions were defined, one based on the ultimate roof displacement ($D_{roof,u}$) and the other on the ultimate inter-storey drift ($\delta_{max\,,u}$). $D_{roof,u}$ was determined through pushover analysis, under a modal pattern of lateral load, and is the roof displacement when the first plastic hinge in a column reaches the collapse rotation. This value is $D_{roof,u}$=0.145 m. $\delta_{max\,,u}$, which is to be compared with the demand evaluated in terms of maximum drift along the height of the building, was determined through pushover analysis and is the maximum drift along the height when the first plastic hinge in a column reaches the collapse rotation. Since a column sway mechanism at the fourth storey was observed during the pushover analysis, the drift corresponds to the ultimate drift of the fourth storey, equal to 2.5375%. It should also be noted that, during the nonlinear dynamic analyses, a column sway mechanism was observed at the third or fourth storey in almost all the cases when the collapse had been reached.

The variability of the annual probability of failure is then examined. With regards to the first order approximation of the hazard curve, the results for $D_{roof,u}$ are reported in Table 8. This table shows the values of probability together with the corresponding values of hazard and dispersion. It can be observed that, under the same conditions of structure and dispersion, the values of annual probability of failure vary considerably, depending on the hazard curve (a) or (b). It can also be seen that, for the same hazard curve (a) or (b), a variation in the dispersion seems to have a greater influence on the final value of the annual probability of failure, including when a comparison was made with a variation to the hazard value. In addition, on examining the parameter of constant dispersion, a much greater annual probability of failure was obtained for the structure without dampers than for the structure with dampers. This, however, does not always occur when the parameter of variable dispersion is used, as in Case 2, see hazard curve (b). The same observations can be made for the collapse defined by $\delta_{max\,,u}$ (not shown) with the additional consideration that, when the variable dispersion parameter (β_{regr}) is used, the annual probability of failure is much greater for the structure with dampers than for the structure without. Consequently, the results are in line with expectations mainly when the parameter of constant dispersion (β_{cost}) is used. Table 8 also gives the values of collapse probability obtained for Case 3 when using the median curves of D_{roof} estimated through the direct assessment method [18] and either the values of dispersion (β_{cost}) or the expressions of dispersion (β_{regr}) derived from the nonlinear dynamic analyses. The values of probability with IDAM were seen to be greater than those obtained from the nonlinear dynamic analyses, and this was due to the conservative estimates obtained for the median curves of D_{roof} and to the different trends of such curves.

When looking at the second order approximation of the hazard curve, for both the demand parameters and for the same structure, there is a smaller difference between the values of $H(S_{a,1}^{NC})$ determined by using different intervals for interpolating the hazard curve (criterion (a) or (b)) than for the first order approximation. This is shown in Table 9 for $D_{roof,u}$ and Case 3. As a consequence, when considering the second order approximation of the hazard curve, the variation, for the same structure and dispersion, of the annual failure probability using the values of $T_{R,}$, is reduced, if compared with the same variation obtained using the first order approximation. Moreover, considering the second order approximation of the hazard curve, the dispersion has a lower influence on the annual failure probability than with the first order approximation. Finally, it is possible to observe that, considering the second order approximation and using both the dispersion parameters, the results are in line with expectations, i.e. the annual failure probability for the structure without dampers is always much greater than that obtained for the structure with dampers.

Table 9
Annual failure probability for different hazard curve approximations, for collapse defined by $D_{roof,u}$ ($D_{roof,u}$=0.145 m) and for Case 3.

	a) I order	a) II order	b) I order	b) II order
With dampers: $S_{a,1}^{NC}$ =0.6144 g, a=0.2421, b=1.0523, β_C=0.275				
$H(S_{a,1}^{NC})$	$1.2{\cdot}10^{-4}$	$3.8{\cdot}10^{-5}$	$4.9{\cdot}10^{-5}$	$1.7{\cdot}10^{-5}$
β_{regr} =0.6717				
$P_{F,NC}$	$7.9{\cdot}10^{-4}$	$7.19{\cdot}10^{-4}$	$2.37{\cdot}10^{-3}$	$4.99{\cdot}10^{-4}$
β_{cost} =0.4696				
$P_{F,NC}$	$3.5{\cdot}10^{-4}$	$2.49{\cdot}10^{-4}$	$4.37{\cdot}10^{-4}$	$2.20{\cdot}10^{-4}$
Without dampers: $S_{a,1}^{NC}$ =0.3763 g, a=0.44, b=1.1357, β_C =0.275				
$H(S_{a,1}^{NC})$	$4.8{\cdot}10^{-4}$	$3.7{\cdot}10^{-4}$	$3.6{\cdot}10^{-4}$	$3.4{\cdot}10^{-4}$
β_{regr} =0.6486				
$P_{F,NC}$	$2.2{\cdot}10^{-3}$	$2.4{\cdot}10^{-3}$	$8.2{\cdot}10^{-3}$	$1.3{\cdot}10^{-3}$
β_{cost} =0.5651				
$P_{F,NC}$	$1.6{\cdot}10^{-3}$	$1.8{\cdot}10^{-3}$	$4.3{\cdot}10^{-3}$	$1.2{\cdot}10^{-3}$

6. Conclusions

Several investigations were performed, by means of nonlinear dynamic analyses, on the application of the simplified SAC-FEMA approach used in the probabilistic seismic assessment of RC structures with and without viscous dampers. The main results are summarized in the following. As expected, the median values obtained for the structure without dampers are greater than those obtained for the structure with dampers, regardless of the number of records considered. Regarding the application of the direct assessment method as an alternative to nonlinear dynamic analyses, the estimates derived from the method for the median curves of D_{roof} are consistent with the results of the nonlinear dynamic analyses. These results show that the method is effective and can be used as a simplified alternative to nonlinear dynamic analyses for probabilistic assessment purposes.

With reference to the dispersion parameter β_{regr}, it is possible to

notice several aspects. Dispersion increases with seismic intensity, it depends on the results of the nonlinear dynamic analyses and, in particular, on the number of records. The expected trend, i.e. greater dispersion for the structure without dampers than for the structure with dampers, was determined only for the higher number of records (180 records). Regarding the dispersion parameter β_{cost}, the trend was as expected even when using a lower number of records. Additionally, β_{cost} increases with the number of seismic events for both the structure with and without dampers. The relationships between the expressions for β_{cost} and β_{regr} for the structure with and without dampers were derived with the purpose of obtaining the dispersion for the structure with dampers, if that for the structure without dampers is known.

With regards to the simplified formula to determine the annual probability of failure $P_{F,\ NC}$, this formula is particularly sensitive to variations in the hazard curve approximation and dispersion. For the hazard curves determined with the first order approximation, it can be observed that different values of $P_{F,\ NC}$ were obtained by changing the interval in which the hazard curve is interpolated. Moreover, the simplified formula for $P_{F,\ NC}$ is particularly affected by dispersion. The values for $P_{F,\ NC}$ were always in line with expectations only when obtained using the parameter of dispersion β_{cost}. Considering the second order approximation of the hazard curve, the variation in the annual failure probability, when changing the interval for interpolating the hazard curve, is reduced if compared to the same variation obtained with the first order approximation. Using the second order approximation, the influence of the values of dispersion is also reduced, and $P_{F,\ NC}$ is always greater for the structure without dampers than for the structure with dampers. The suggestion, therefore, is to use the parameter of constant dispersion β_{cost} when considering the first order approximation for the hazard curve. Otherwise, the second order approximation allows users to obtain values of probability that are less sensitive to the interval for interpolating the hazard curve and to type of dispersion, β_{regr} or β_{cost}.

References

[1] Constantinou MC, Soong TT, Dargush GF. Passive Energy Dissipation Systems for Structural Design and Retrofit [MCEER Monograph no. 1]. Multidisciplinary Center for Earthquake Engineering Research, State University of New York at Buffalo; 1998.

[2] Ramirez OM, Constantinou MC, Kirche CA, Whittaker AS, Johnson MW, Gomez JD, Chrysostomou CZ. Development and evaluation of simplified procedures for analysis and design of buildings with passive energy dissipation systems [Report MCEER-00-0010]. State University of New York at Buffalo; 2000.

[3] Miyamoto K, Taylor D, Duflot F. Seismic rehabilitation of a reinforced concrete hotel using fluid viscous dampers. In: Proceedings of the 12th European Conference on Earthquake Engineering, London, UK; 2002.

[4] Christopoulos C, Filiatrault A. Principles of Passive Supplemental Damping and Seismic Isolation. Pavia, Italy: IUSS Press; 2006.

[5] Sorace S, Terenzi G. Seismic protection of frame structures by fluid viscous damped braces. ASCE J Struct Eng 2008;134:45–55.

[6] Mazza F, Vulcano A. Control of the earthquake and wind dynamic response of steel-framed buildings by using additional braces and/or viscoelastic dampers. Earthq Eng Struct Dyn 2011;40:155–74.

[7] Sullivan TJ, Lago A. Towards a simplified Direct DBD procedure for the seismic design of moment resisting frames with viscous dampers. Eng Struct 2012;35:140–8.

[8] Palermo M, Silvestri S, Trombetti T, Landi L. Force reduction factor for building structures equipped with added viscous dampers. Bull Earthq Eng 2013;11(5):1661–81.

[9] Palermo M, Muscio S, Silvestri S, Landi L, Trombetti T. On the dimensioning of viscous dampers for the mitigation of the earthquake-induced effects in moment-resisting frame structures. Bull Earthq Eng 2013;11(6):2429–46.

[10] Landi L, Lucchi S, Diotallevi PP. A procedure for the direct determination of the required supplemental damping for the seismic retrofit with viscous dampers. Eng Struct 2014;71:137–49.

[11] Benedetti A, Landi L, Merenda DG. Displacement-based design of an energy dissipating system for seismic upgrading of existing masonry structures. J Earthq Eng 2014;18:477–501.

[12] Landi L, Conti F, Diotallevi PP. Effectiveness of different distributions of viscous damping coefficients for the seismic retrofit of regular and irregular RC frames. Eng Struct 2015;100:79–93.

[13] Porter KA. An Overview of PEER's Performance-Based Earthquake Engineering Methodology. In: Proceedings of the Ninth International Conference on Applications of Probability and Statistics in Engineering, San Francisco, California, USA; 2003.

[14] FEMA P-58 . Seismic Performance Assessment of Buildings: vol. 1 – Methodology [FEMA P-58-1]. Washington D.C., USA: Prepared by the Applied Technology Council for the Federal Emergency Management Agency; 2012.

[15] Cornell CA, Jalayer F, Hamburger RO, Foutch DA. Probabilistic basis for 2000 SAC federal emergency management agency steel moment frame guidelines. J Struct Eng 2002;128(4):526–33.

[16] Dolšek M, Fajfar P. Simplified probabilistic seismic performance assessment of plan-asymmetric buildings. Earthq Eng Struct Dyn 2007;36(13):2021–41.

[17] Welch DP, Sullivan TJ, Calvi GM. Developing displacement-based procedures for simplified loss assessment in performance-based earthquake engineering. J Earthq Eng 2014;18(2):290–322.

[18] Landi L, Fabbri O, Diotallevi PP. A two-step direct method for estimating the seismic response of nonlinear structures equipped with nonlinear viscous dampers. Earthq Eng Struct Dyn 2014;43:1641–59.

[19] FEMA 350 . Recommended Seismic Design Criteria for New Steel Moment Frame Buildings [SAC Joint Venture]. Washington D.C., USA: FEMA; 2000.

[20] Diotallevi PP, Landi L, Dellavalle A. A methodology for the direct assessment of the damping ratio of structures equipped with nonlinear viscous dampers. J Earthq Eng 2012;16(3):350–73.

[21] Min LLPP. Norme Tecniche per le Costruzioni. Italian building code, adopted with D.M. 14/01/2008, published on S.O. n. 30 G.U. n. 29, 04/02/2008; 2008.

[22] Iervolino I, Galasso C, Cosenza E. REXEL: computer aided record selection for code-based seismic structural analysis. Bull Earthq Eng 2010;8(2):339–62.

[23] Ambraseys NN, Smit P, Douglas J, Margaris B, Sigbjörnsson R, Ólafsson S, Suhadolc P, Costa G. Internet site for European strong-motion data. Boll Geofis Appl Teor 2004;45(3):113–29.

[24] CSI . Analysis Reference Manual for SAP2000. Berkeley, California, USA: ETABS, and SAFE; 2009.

[25] Min LLPP. Circolare 2 febbraio 2009, n. 617. Istruzioni per l'applicazione delle Nuove norme tecniche per le costruzioni. Commentary to the Italian building code, adopted with D.M. 14/01/2008, published on S.O. n. 27 G.U. n. 47, 26/02/2009.

[26] Panagiotakos TB, Fardis MN. Deformations of reinforced concrete members at yielding and ultimate. ACI Struct J 2001;98(2):135–48.

[27] Bommer JJ, Elnashai AS, Weir AG. Compatible acceleration and displacement spectra for seismic design codes. In: Proceedings of the 12th World Conference on Earthquake Engineering, Auckland, New Zealand; 2000.

[28] Vamvatsikos D. Derivation of new SAC/FEMA performance evaluation solutions with second-order hazard approximation. Earthq Eng Struct Dyn 2013;42:1171–88.